ORGANOMETALLICS

pubs.acs.org/Organometallics Article

# Examination of a Series of Ir and Rh PXL Pincer Complexes as (Pre)catalysts for Aromatic C−H Borylation

Ming-Uei Hung, Loren P. Press, Nattamai Bhuvanesh, and Oleg V. Ozerov*

Cite This: *Organometallics* 2021, 40, 1004−1013 Read Online

ACCESS | Metrics & More | Article Recommendations | Supporting Information

**ABSTRACT:** This work follows a previously published study of high-turnover aromatic C−H borylation by Ir complexes supported by POCOP-type ligands incorporating $-P^iPr_2$ side donors (**L1**−**L3**) using HBpin in the presence of olefins. A variety of pincer-supported Ir and Rh complexes have been tested as precatalysts in the analogous aromatic C−H borylation. The ligands in this study included a number of aryl/bis(phosphine) pincers of the PCP type, as well as PCS, PNP, PNSb, PSiP, and PBP ligands. The syntheses primarily targeted precursors of the (PXL)M(H)(Cl) type (M = Rh, Ir); exceptions included complexes (**L15**)Ir(H)(OAc), (**L17**)Ir(COE), (**L18**)Ir(H)$_4$, and (**L16**)Rh(H$_2$). The catalytic competence was tested using $C_6D_6$ as the substrate (and solvent) with HBpin and 1-hexene as reagents. C−H borylation and hydroboration of 1-hexene were the two competing catalytic reactions. None of the Rh complexes tested displayed any C−H borylation activity. Among the Ir complexes, only those possessing a central aryl site in the pincer showed significant C−H borylation activity with $C_6D_6$. The most promising precatalysts (**L3**)Ir(H)(Cl), (**L4**)Ir(H)(Cl), (**L7**)Ir(H)(Cl), (**L11**)Ir(H)(Cl), (**L13**)Ir(H)(Cl), and (**L15**)Ir(H)(OAc) were tested in the C−H borylation of $C_6H_5F$ and $C_6H_5CF_3$. All of these catalysts showed a roughly statistical preference for the borylation of only *meta* and *para* sites in $C_6H_5CF_3$. For $C_6H_5F$ borylation of all three sites (*ortho*, *meta*, *para*) was observed. Catalysts supported by the ligands **L3** and **L11** showed the highest rate of reaction and higher selectivity for C−H borylation vs hydroboration. Borylation of *m*-$ClC_6H_4Me$ catalyzed by (**L3**)Ir(H)(Cl) and (**L11**)Ir(H)(Cl) resulted in only the borylation of only one aromatic C−H site (*meta* to both substituents), <10% of borylation of the benzylic site, and no borylation of the C−Cl moiety.

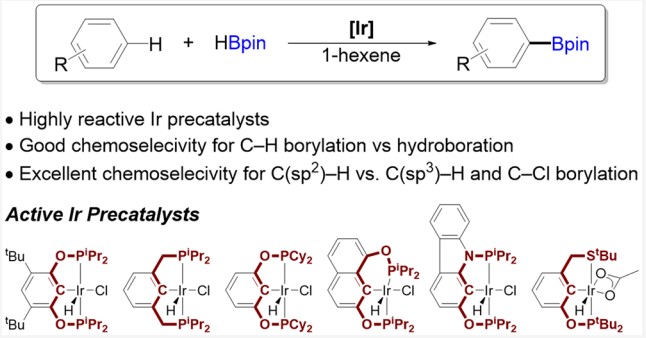


## INTRODUCTION

The synthesis of derivatives of organoboronic acids[1] via homogeneous catalysis of C−H bond borylation (Scheme 1A) is an attractive method of preparation of versatile synthetic building blocks.[2−5] The most impressive foundational successes in this chemistry have been associated with catalysis of aromatic C−H borylation by Ir complexes supported by neutral bidentate ligands.[6−8] Catalytic borylation of aromatic and other sp$^2$ and sp$^3$ C−H bonds has also been realized with a variety of transition-metal and main-group complexes.[9−25] Our group has reported on the catalysis of dehydrogenative borylation of the sp C−H bonds in terminal alkynes (DHBTA) using Ir complexes supported by diarylamido-centered SiNN[26,27] or PNP[28−31] pincer[32−36] ligands. Catalysis of DHBTA with other metals has also been reported,[37−41] but the activity and the chemoselectivity of the Ir catalysts are superior.

In 2016, we reported catalysis of aromatic C−H borylation with HBpin by Ir complexes supported by different, POCOP-type, pincer ligands.[42] (Scheme 1B) These catalysts were capable of >10$^4$ turnovers, rivaling the activity of the best Ir catalysts supported by bidentate ligands. Interestingly, the (POCOP)Ir catalysis proceeded by a different mechanism (Scheme 1C), which required the use of a sacrificial olefin for kinetic reasons.[42,43] This is in contrast to the catalysis by the bidentate-ligand-supported Ir, which does not require and is indeed poisoned by simple olefins. It should also be noted that the SiNN- and PNP-supported Ir pincer catalysts for DHBTA do not catalyze aromatic C−H borylation and furthermore operate by different mechanisms in DHBTA.[27,31] On the whole, there exists a remarkable mechanistic diversity of possible C−H borylation pathways with Ir, depending on the supporting ligands and the substrate.

We wished to expand on our 2016 study and examine a wide array of PXP/PXL pincer ligands as aromatic C−H borylation catalysts, potentially targeting improved selectivity and activity.

**Received:** February 9, 2021
**Published:** March 29, 2021

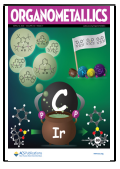







https://doi.org/10.1021/acs.organomet.1c00081
*Organometallics* 2021, 40, 1004−1013

**Scheme 1. (A) Catalytic C−H Borylation using HBpin or $B_2pin_2$, (B) (POCOP)Ir-Catalyzed Arene C−H Borylation, and (C) Proposed Reaction Mechanism of (POCOP)Ir-Catalyzed Arene C−H Borylation**

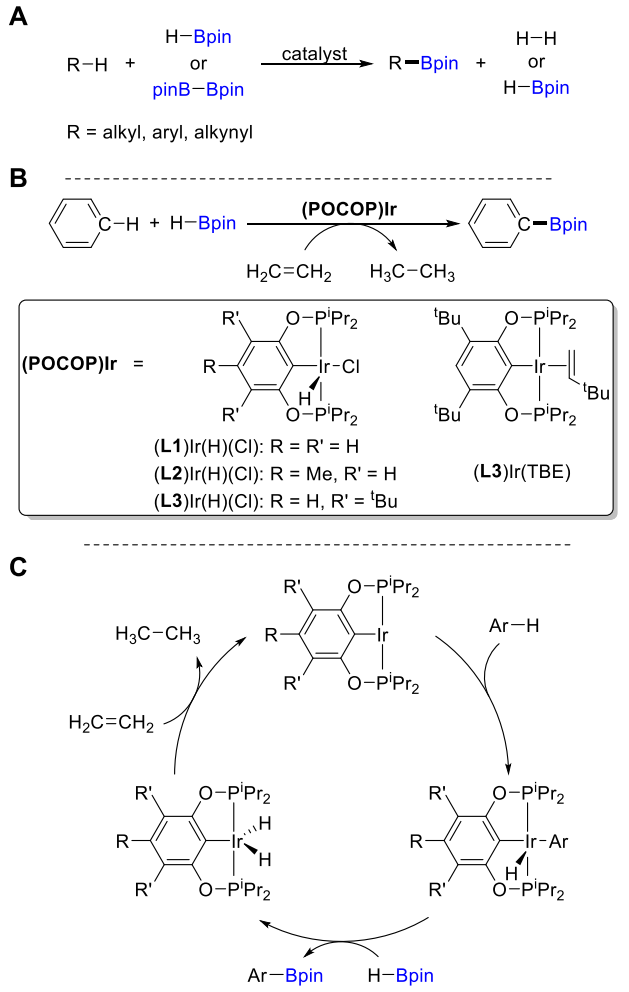


In addition, we tested some analogous pincer complexes of Rh. The present report documents the results of our study.

## RESULTS AND DISCUSSION

**Synthesis of Pincer Ligands.** We set out to examine a variety of ligands with a central aryl group, as well as ligands that possess other central anionic donors based on B, N, or Si (**L3-H**−**L19-H**, Figure 1). Ligands **L3**−**L14** have phosphines as L-type arm donors and an aryl site as an X-type central donor (PCP ligands). The series of ligands was selected to explore steric and electronic variations in the PCP pincer structure. Ligand **L15** was chosen to compare a sulfur donor to a phosphorus donor and also to examine the steric effect of three $^t$Bu groups about the metal as opposed to four $^i$Pr or four $^t$Bu groups. Ligands **L16**−**L19** were chosen to test the viability of different X-type central donors: amido, boryl, and silyl.

**L3-H**,[42] **L5-H**,[44] **L6-H**,[41] **L8-H**,[45] **L9-H**,[45] **L10-H**,[46] **L11-H**,[47] **L12-H**,[47] **L13-H**,[48] **L14-H**,[48] **L16-H**,[49] **L17-H**,[50] **L18-Ph**,[51] and **L19-H**[43] have been previously reported and were synthesized as described in the literature. **L4-H** was prepared from 1,3-resorcinol, chlorodicyclohexylphosphine, and triethylamine as a base. **L7-H** was prepared analogously from 2-hydroxycarbazole, chlorodiisopropylphosphine, and *n*-butyllithium as a base. **L7-H** contained two isomers in a ca. 1:1 ratio. In the $^{31}P\{^1H\}$ NMR spectrum in $C_6D_6$ at room temperature, four $^{31}P$ NMR resonances were observed. $^{31}P$ NMR resonances at $\delta$ 148.7 and 147.9 were assigned to P−O of two isomers, respectively, and $^{31}P$ NMR resonances at $\delta$ 61.2 and 60.6 were assigned to P−N of two isomers, respectively. The $^1H$ NMR spectrum also showed two sets of resonances that correspond to two isomers. The nature of the two isomers was not determined, but we tentatively assume that these are rotamers arising from restricted rotation associated with the N−P and/or C−O−P bonds. **L15-H** was synthesized from 3-hydroxybenzyl alcohol. 3-Hydroxybenzyl alcohol **1** was chlorinated with thionyl chloride and pyridine to provide 3-hydroxybenzyl chloride **2**. **2** was treated with *n*-butyllithium and $ClP^tBu_2$ to provide compound **3**. **3** was then treated with sodium *tert*-butylthiolate to provide **L15-H** (Scheme 2).

**Synthesis of Ir and Rh Pincer Complexes.** All of the pincer complexes in this study are shown in Figure 2. The pincer complexes of Rh, (**L3**)Rh(H)(Cl),[52] (**L16**)Rh($H_2$),[53] and (**L18**)Rh(H)(Cl),[51] were prepared as previously described. Literature procedures were also used to obtain Ir complexes with central donors other than aryl, (**L16**)Ir(H)(Cl),[54] (**L17**)Ir(COE)[50] and (**L18**)Ir$(H)_4$,[55] and (**L19**)Ir(H)(Cl).[43]

Installation of the PCP ligands into the coordination sphere of Ir is most conveniently accomplished via reaction of the ligand precursor with $[(COD)IrCl]_2$ (COD = 1,5-cyclooctadiene) or $[(COE)_2IrCl]_2$. The insertion of a metal center into the central aromatic C−H bond and the loss of the olefin placeholder ligand, COD and COE, can ideally lead to the five-coordinate Ir(III) complex (**L**)Ir(H)(Cl) (Scheme 3, method A). However, method A does not always provide for the clean formation of the desired product; therefore, different strategies were sampled to access the desired (**L**)Ir complexes.

Reacting $[(COD)IrCl]_2$ or $[(COE)_2IrCl]_2$ with pyridine prior to the addition of the ligand precursor results in the formation of a pyridine adduct, (**L**)Ir(H)(Cl)(py) (Scheme 3, method B). The pyridine ligand can then be abstracted with boron trifluoride diethyl etherate ($BF_3{\cdot}OEt_2$) to give the desired five-coordinate complex (**L**)Ir(H)(Cl). This approach has been reported to access clean (POCOP)Ir and (POCOP)Rh complexes.[42,48,56] Alternatively, $[(COD)M(OAc)]_2$ (M = Ir, Rh) was also used in the metalation of the pincer ligands to yield the products (**L**)Ir(H)(OAc).[30,48] The $\kappa^2$-acetate ligand provides protection to the sixth coordination site of the Ir center (Scheme 3, method C). Another approach (Scheme 3, method D) was described by Waterman and co-workers, who reported that the reaction of the ligand precursor **L1-H** with $[(COE)_2IrCl]_2$ under an atmosphere of $H_2$ gave a high yield of (**L1**)Ir(H)(Cl).[57]

Methods A−D were then screened for the metalation of a ligand on the 10−100 $\mu$mol scale (Table 1). Ir complexes (**L3**)Ir(H)(Cl),[42] (**L4**)Ir(H)(Cl), (**L5**)Ir(H)(Cl),[44] (**L7**)Ir(H)(Cl), (**L16**)Ir(H)(Cl),[54] and (**L19**)Ir(H)(Cl)[43] were successfully formed via method A. Using method B, (**L8**)Ir(H)(Cl)(py) and (**L13**)Ir(H)(Cl)(py) were successfully formed. (**L15**)Ir(H)(OAc) was formed cleanly by using method C. Method D was used to yield (**L4**)Ir(H)(Cl) and (**L11**)Ir(H)(Cl). Unfortunately, we were not able to optimize the syntheses or isolation of the desired Ir products from the reactions using **L6-H**, **L9-H**, **L10-H**, **L12-H**, and **L14-H**.

Scheme 4 shows the syntheses of new Ir complexes (top) and the improved syntheses of (**L11**)Ir(H)(Cl) and (**L11**)Rh(H)(Cl) (bottom) on a preparative scale. (**L11**)Ir(H)(Cl) and


https://doi.org/10.1021/acs.organomet.1c00081
Organometallics 2021, 40, 1004−1013

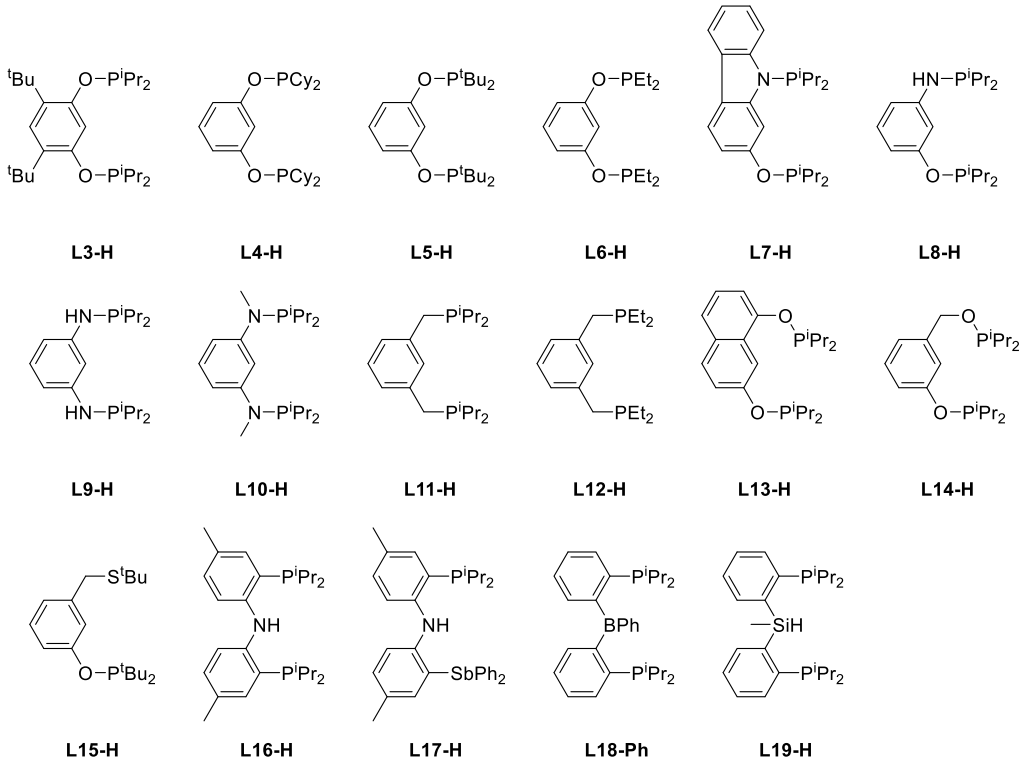


**Figure 1.** LXL-type ligands used in this study.

**Scheme 2. Synthesis of L4-H, L7-H, and L15-H**

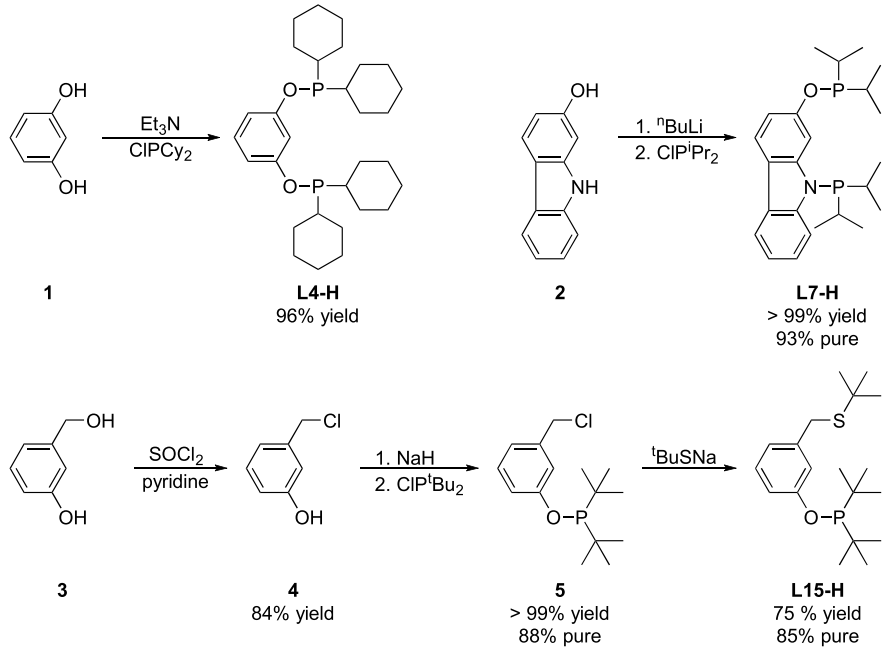


(**L11**)Rh(H)(Cl) have been previously accessed via method A in low yields and with difficult workup.[28,48] The use of method D allowed isolation of these compounds in excellent yields from a single step. (**L4**)Ir(H)(Cl), (**L7**)Ir(H)(Cl), (**L8**)Ir(H)(Cl)(py), (**L13**)Ir(H)(Cl)(py), and (**L15**)Ir(H)(OAc) were then prepared in moderate to excellent yields by the best methods on the basis of the screening experiments in Table 1. (**L8**)Ir(H)(Cl)(py) and (**L13**)Ir(H)(Cl)(py) both exist as a pair of isomers, related by the exchange of positions of py and Cl about the octahedral Ir (Figure 3). Abstraction of pyridine from (**L8**)Ir(H)(Cl)(py) and (**L13**)Ir(H)(Cl)(py) was attempted by reacting with $BF_3{\cdot}OEt_2$. The "pyridine-free" unsaturated Ir complexes (**L8**)Ir(H)(Cl) and (**L13**)Ir(H)(Cl) were observed in the reaction mixture with excess $BF_3{\cdot}OEt_2$, as well as the expected byproduct $BF_3$py. The pentane-soluble (**L13**)Ir(H)(Cl) was then successfully isolated in 54% yield. However, attempts at isolation of (**L8**)Ir(H)(Cl) from the reaction mixture were not successful due to the similar solubilities of (**L8**)Ir(H)(Cl) and $BF_3$py. Neither recrystallization nor reprecipitation from toluene, pentane, or mixed solvents was


https://doi.org/10.1021/acs.organomet.1c00081
Organometallics 2021, 40, 1004−1013

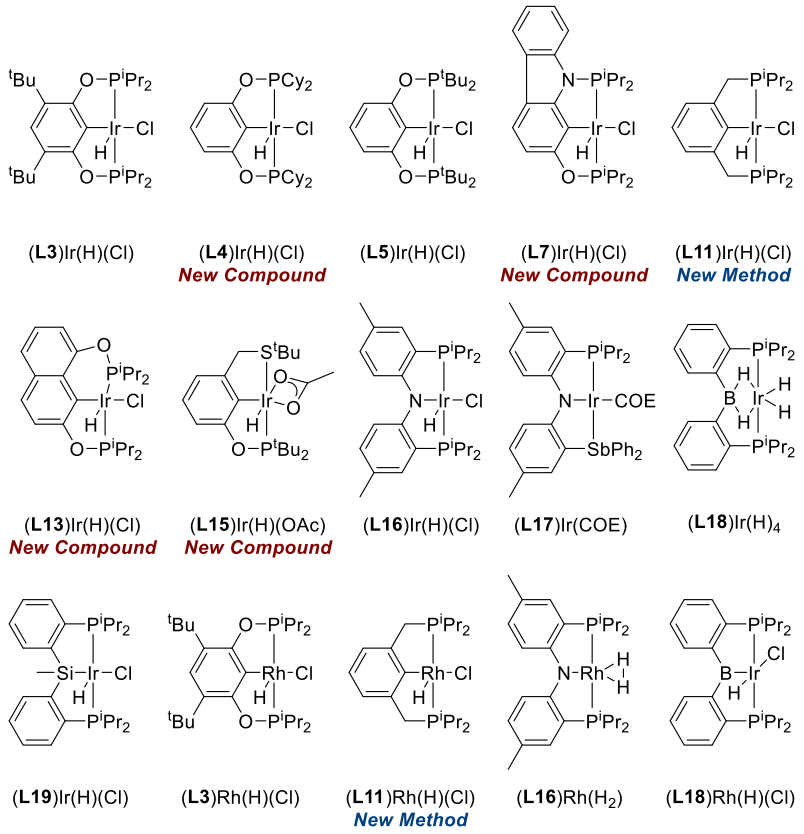


**Figure 2.** Pincer complexes of Ir and Rh in this study.

**Scheme 3. Different Methods for Metalation of LXL-Type Ligands**

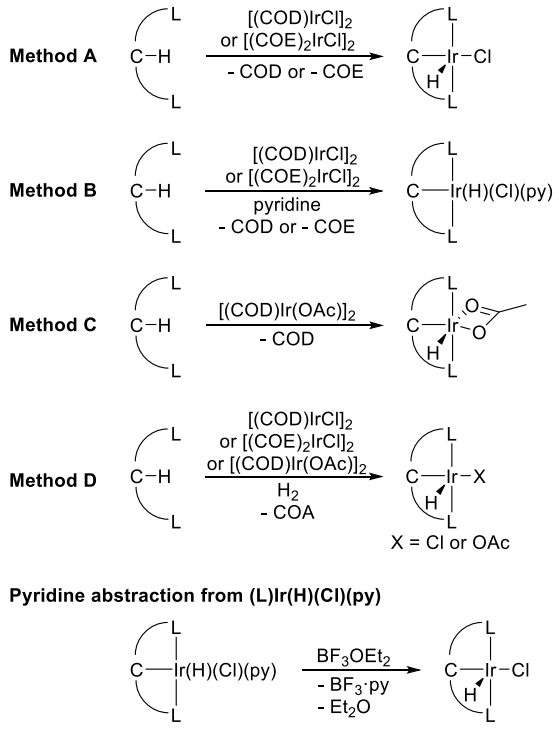


successful. Using THF or column chromatography on silica gel to separate (**L8**)Ir(H)(Cl) from $BF_3$py resulted in the regeneration of (**L8**)Ir(H)(Cl)(py). The preparation of (**L**)Ir(H)(Cl) method B (+ pyridine abstraction) seemed to work only if the resulting (**L**)Ir(H)(Cl) and $BF_3$py have a dramatic solubility difference.

The newly synthesized complexes (**L4**)Ir(H)(Cl), (**L7**)Ir(H)(Cl), (**L13**)Ir(H)(Cl), and (**L15**)Ir(H)(OAc) were characterized by $^1$H, $^{13}$C{$^1$H}, and $^{31}$P{$^1$H} NMR spectroscopy and elemental analysis. (**L8**)Ir(H)(Cl)(py), (**L8**)Ir(H)(Cl), and (**L13**)Ir(H)(Cl)(py) were characterized by $^1$H and $^{31}$P{$^1$H} NMR spectroscopy. The $^1$H NMR chemical shifts for Ir−H and $^{31}$P{$^1$H} NMR chemical shifts are given in Table 2.

**X-ray Structural Study.** The solid-state structure of (**L15**)Ir(H)(OAc) was determined by single-crystal X-ray diffraction methods (Figure 4). As expected, the pincer ligand **L15** is bound meridionally (P1−Ir1−S1 = 164.61(3)°) to the Ir center. One of the oxygen atoms (O2) in the $\kappa^2$-acetate is *trans* to the central aryl carbon (C1), and another oxygen atom (O3) is *trans* to the implied hydride ligand. The Ir1−O3 bond (2.296(2) Å) *trans* to the hydride is longer than the Ir1−O2 bond (2.211(2) Å) *trans* to $C_{aryl}$. The *tert*-butyl group on the sulfur donor is *syn* to the hydride ligand.

**Catalysis of Aromatic C−H Borylation.** We then screened the catalytic activity of the Ir and Rh complexes in the aromatic C−H borylation. In our previous report, both 1-hexene and ethylene allowed efficient catalysis with (**L3**)Ir(H)(Cl).[42] In this study, we selected 1-hexene for its operational simplicity in the J. Young NMR tube experiments. The reaction progress was followed by $^1$H NMR spectroscopy using cyclohexane as an internal standard. The model reaction used HBpin as the


https://doi.org/10.1021/acs.organomet.1c00081
Organometallics 2021, 40, 1004−1013

**Table 1. Screening of Methods for Metalation of LXL-Type Pincer Ligands**[a]

| ligand | method A | method B | method C | method D |
|---|---|---|---|---|
| **L3-H** | ○[42] | – | – | – |
| **L4-H** | ○ | – | – | ○ |
| **L5-H** | ○[44] | – | – | – |
| **L6-H** | – | × | × | × |
| **L7-H** | △ with $[(COD)IrCl]_2$ | △ | – | – |
| | ○ with $[(COE)_2IrCl]_2$ | △ | – | – |
| **L8-H** | ▲ with $[(COD)IrCl]_2$ | ○ | △ | △ |
| | △ with $[(COE)_2IrCl]_2$ | ○ | △ | △ |
| **L9-H** | △ | △ | × | × |
| **L10-H** | × | × | × | × |
| **L11-H** | ▲[28] | – | – | ○ |
| **L12-H** | – | × | × | × |
| **L13-H** | × | △ with $[(COD)IrCl]_2$ | × | × |
| | × | ○ with $[(COE)_2IrCl]_2$ | × | × |
| **L14-H** | × | × | × | × |
| **L15-H** | × | – | ○ | × |
| **L16-H** | ○[54] | – | – | – |
| **L17-H**[58] | – | – | – | – |
| **L18-Ph** | ○[51,59] | – | – | – |
| **L19-H** | ○[43] | – | – | – |

[a]Legend: ○, desired product formed as the only product; △, desired product formed as a major product (>50%); ▲, desired product was observed as a minor product (<50%); ×, desired product was not observed or identified; –, did not test.

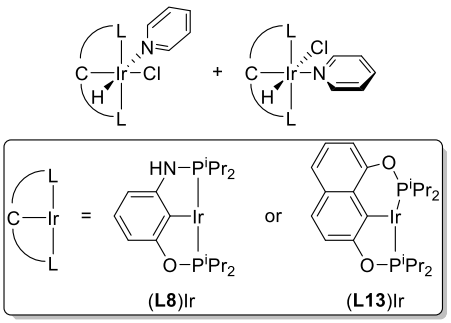


**Figure 3.** Two configurational isomers in (**L8**)Ir(H)(Cl)(py) and (**L13**)Ir(H)(Cl)(py).

limiting reagent, 25 equiv of $C_6D_6$ as the substrate, 1 mol % precatalyst loading, and 3 equiv of 1-hexene.

The screening results are summarized in Table 3. Ir complexes bearing PXL-type pincer ligands with an aryl carbon as a central donor, except for (**L5**)Ir(H)(Cl), catalyzed aromatic C–H borylation with moderate to good chemoselectivity over the competing hydroboration side reaction (Table 3, entries 1–7). (**L5**)Ir(H)(Cl) only catalyzed hydroboration of 1-hexene (Table 3, entry 3). Ir complexes supported by the PBP, PNP, PNSb, and PSiP ligands did not show catalytic activity for aromatic C–H borylation; they did catalyze hydroboration (Table 3, entries 8–11). The Rh complexes also did not catalyze C–H borylation (Table 3, entries 12–15). We have also conducted the reaction without 1-hexene (see the Supporting Information). Without 1-hexene, none of the reactions gave any detectable formation of $C_6D_5Bpin$.

After identification of the promising complexes (**L3**)Ir(H)(Cl), (**L4**)Ir(H)(Cl), (**L7**)Ir(H)(Cl), (**L11**)Ir(H)(Cl), (**L13**)Ir(H)(Cl), and (**L15**)Ir(H)(OAc) for aromatic C–H borylation, (**L11**)Ir(H)(Cl) was chosen as a precatalyst to further examine different reaction conditions because of its best reactivity and chemoselectivity. First, we identified that 1-hexene is a promising $H_2$ acceptor. Table 4 summarizes the results when various olefins were used in comparison to 1-hexene. Bulky *tert*-butylethylene and internal alkenes did not provide the desired reactivity (Table 4, entries 2–4). Next we investigated the effect of the reagent ratio on the reactivity and chemoselectivity, and the results are summarized in Table 5. A large excess of arene is crucial for good chemoselectivity (Table 5, entries 4–6 vs entries 1–3). The chemoselectivity was not much affected by the amount of 1-hexene added when more than 2 equiv of 1-hexene was used. However, using 3 equiv of 1-hexene allowed completion of the reaction within 19 h, while up to 38 h was required when 2 equiv of 1-hexene was used (Table 5, entries 3 and 6 vs entries 2 and 5). These results are consistent with the previously reported aromatic C–H borylation by (POCOP)Ir complexes.[42]

With the optimized conditions in hand, we then tested the regioselectivity of the catalysis using complexes (**L3**)Ir(H)(Cl), (**L4**)Ir(H)(Cl), (**L7**)Ir(H)(Cl), (**L11**)Ir(H)(Cl), (**L13**)Ir(H)(Cl), and (**L15**)Ir(H)(OAc). The regioselectivity of aromatic C–H borylation catalyzed by pincer and non-pincer catalysts in the previously reported examples is mainly sterically controlled.[4,42] Borylation of monosubstituted benzenes generally gives the *meta*- and *para*-borylated products in a nearly 2:1 ratio.[4,42] Exceptions are those arenes with small electronegative substituents, such as fluorobenzene and anisole, which give rise to *ortho* borylation as well.[4,42] When (**L2**)Ir(H)(Cl) was used as a precatalyst in our 2016 study, borylation of fluorobenzene with 0.03 mol % precatalyst loading at 80 °C for 24 h under an atmosphere of ethylene gave a borylated product mixture in 45% yield (*ortho*/*meta*/*para* = 40/46/14).[42] The same conditions for the borylation of benzotrifluoride gave a mixture of borylated products in total 43% yield (*ortho*/*meta*/*para* = 0/70/30).[42] In this study, we selected fluorobenzene and benzotrifluoride as model substrates to test the regioselectivity on $sp^2$ C–H bonds when different Ir complexes were used as precatalysts.

Table 6 details the results of the regioselectivity tests in reactions conducted at 80 °C for 24 h with 0.1 mol % precatalyst loading using fluorobenzene and benzotrifluoride, respectively. (**L3**)Ir(H)(Cl) and (**L11**)Ir(H)(Cl) showed the highest reactivity, fully consuming HBpin with 0.1 mol % precatalyst loading in 24 h (Table 6, entries 1, 4, 7, and 10). Reactions catalyzed by (**L11**)Ir(H)(Cl) gave the highest chemoselectivity for C–H borylation over hydroboration of up to 5.8:1. The C–H borylation of fluorobenzene, which has a small fluorine substituent, yielded mixtures of all three possible products; however, different product ratios were observed when (**L11**)Ir(H)(Cl), (**L13**)Ir(H)(Cl), and (**L15**)Ir(H)(OAc) were used in comparison to (**L3**)Ir(H)(Cl) (Table 6, entries 4–6 vs entry 1). The borylation of benzotrifluoride, which has a larger substituent, gave very similar regioselectivity when different precatalysts were used (Table 6, entries 7–12). In addition, we investigated the chemoselectivity of precatalysts (**L3**)Ir(H)(Cl) and (**L11**)Ir(H)(Cl) with regard to the activation of $sp^2$ C–H, $sp^3$ C–H, or C–Cl bonds using 3-chlorotoluene as a test substrate (Scheme 5). In both experiments, C–Cl bonds


https://doi.org/10.1021/acs.organomet.1c00081
Organometallics 2021, 40, 1004–1013

**Scheme 4. Preparative Synthesis of Ir and Rh Complexes**

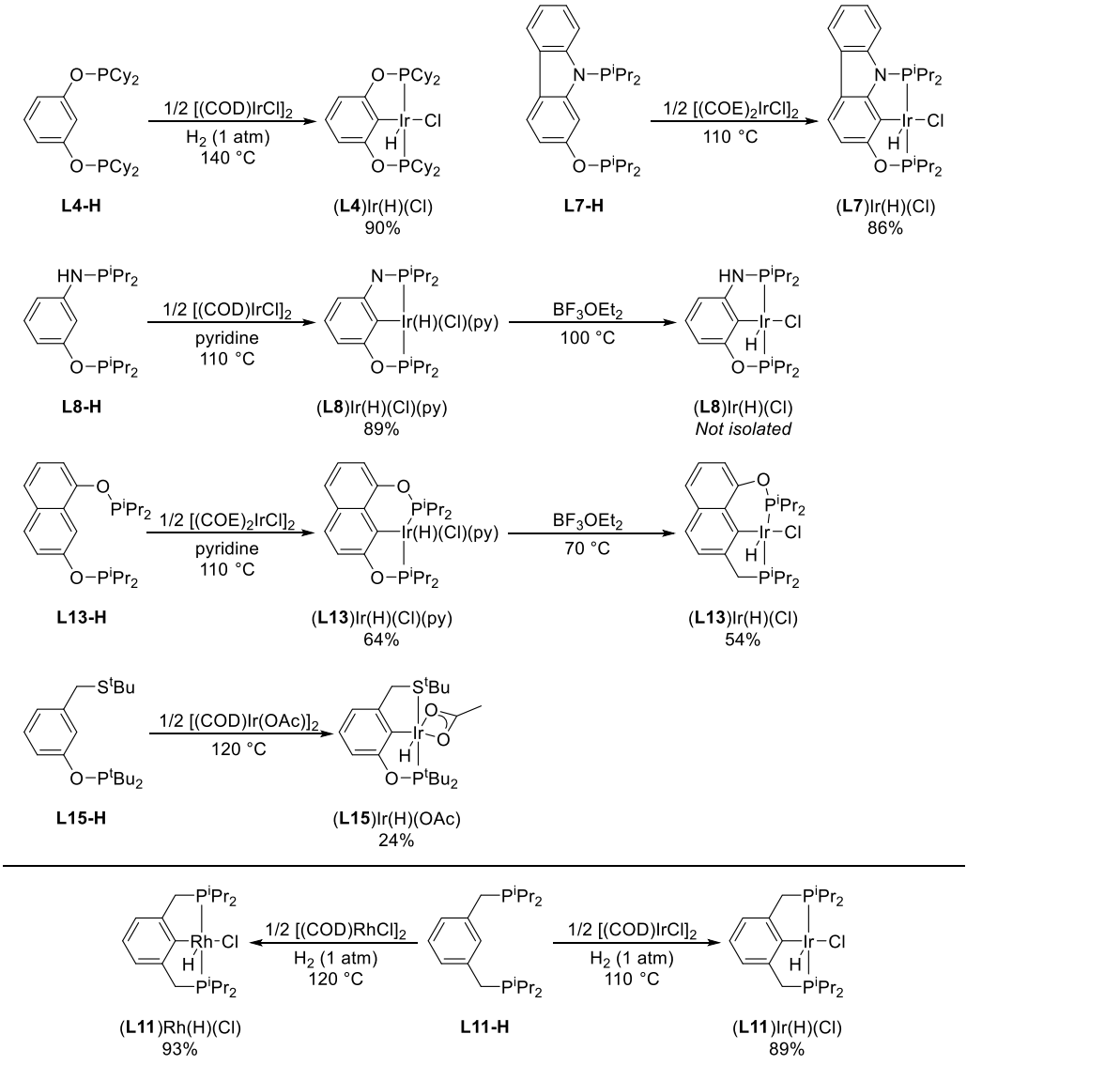


**Table 2. $^{1}$H NMR (Ir−H) and $^{31}$P NMR Chemical Shifts of Ir Complexes**

| | $^{1}$H NMR (Ir−H) (ppm) | $^{31}$P NMR (ppm) | $^{2}J_{P-P}$ (Hz) |
|---|---|---|---|
| (**L3**)Ir(H)(Cl)[42] | −36.6 | 173.5 | |
| (**L4**)Ir(H)(Cl) | −37.25 | 166.7 | |
| (**L7**)Ir(H)(Cl) | −36.77 | 171.1, 115.6 | 373 |
| (**L8**)Ir(H)(Cl)(py) | −21.20 (major) | 147.0, 80.6 (major) | 383 (major) |
| | −21.33 (minor) | 145.2, 80.1 (minor) | 373 (minor) |
| (**L8**)Ir(H)(Cl) | −37.42 | 170.9, 106.0 | 365 |
| (**L13**)Ir(H)(Cl)(py) | −20.74 (major) | 144.6, 120.9 (major) | 406 (major) |
| | −20.42 (minor) | 144.1, 112.0 (minor) | 395 (minor) |
| (**L13**)Ir(H)(Cl) | −36.39 | 172.7, 150.1 | 385 |
| (**L15**)Ir(H)(OAc) | −28.80 | 156.8 | |

remained untouched. (**L11**)Ir(H)(Cl) possessed excellent sp$^2$/sp$^3$ C−H selectivity in a ratio of 35/1, while the selectivity of (**L3**)Ir(H)(Cl) was 5.6/1.

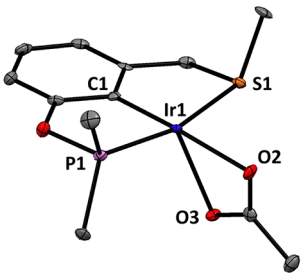


**Figure 4.** ORTEP[60] drawings (50% probability ellipsoids) of (**L15**)Ir(H)(OAc) (CCDC 2041134). Hydrogen atoms and methyl groups of *tert*-butyl arms are omitted for clarity. Selected distances (Å) and angles (deg): Ir1−C1, 1.998(3); Ir1−O2, 2.211(2); Ir1−O3, 2.296(2); P1−Ir1−S1, 164.61(3); O2−Ir1−S1, 91.38(7); O2−Ir1−P1, 103.78(7); C1−Ir1−S1, 83.98(10); C1−Ir1−P1, 81.36(10).

## CONCLUSION

In summary, we have described the synthesis of an array of PXL pincer ligands and their Ir and Rh complexes, including several new compounds. These complexes were then tested as


https://doi.org/10.1021/acs.organomet.1c00081
Organometallics 2021, 40, 1004−1013

**Table 3. Aromatic C−H Borylation Experiments Using Ir or Rh Precatalysts**[a]

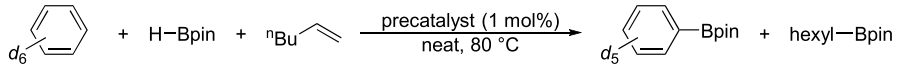


25 equiv 1 equiv 3 equiv

| entry | precatalyst | time (h) | conversion (%)[b] | yield (%)[b] $C_6D_5Bpin$ | yield (%)[b] hexyl-Bpin |
|---|---|---|---|---|---|
| 1 | (**L3**)Ir(H)(Cl) | 1 | 100 | 80 | 19 |
| 2 | (**L4**)Ir(H)(Cl) | 15 | 100 | 89 | 11 |
| 3 | (**L5**)Ir(H)(Cl) | 24 | 100 | 1 | 96 |
| 4 | (**L7**)Ir(H)(Cl) | 3 | 100 | 85 | 13 |
| 5 | (**L11**)Ir(H)(Cl) | 3 | 100 | 89 | 11 |
| 6 | (**L13**)Ir(H)(Cl) | 15 | 94 | 65 | 29 |
| 7 | (**L15**)Ir(H)(OAc) | 15 | 95 | 40 | 45 |
| 8 | (**L16**)Ir(H)(Cl) | 15 | 100 | 2 | 98 |
| 9 | (**L17**)Ir(COE) | 1 | 100 | 0 | 95 |
| 10 | (**L18**)$Ir(H)_4$ | 15 | 100 | 2 | 94 |
| 11 | (**L19**)Ir(H)(Cl) | 15 | 100 | 2 | 98 |
| 12 | (**L3**)Rh(H)(Cl) | 16 | 5 | 0 | 4 |
| 13 | (**L11**)Rh(H)(Cl) | 16 | 16 | 0 | 4 |
| 14[c] | (**L16**)$Rh(H_2)$ | 0.16 | 100 | 0 | 81 |
| 15 | (**L18**)Rh(H)(Cl) | 15 | 88 | 0 | 71 |

[a]Reaction conditions unless specified otherwise: HBpin (36 $\mu$L, 0.25 mmol), 1-hexene (93 $\mu$L, 0.75 mmol), and precatalyst (2.6 $\mu$mol) in $C_6D_6$ (555 $\mu$L, 6.27 mmol), 80 °C, under Ar. [b]Conversions and yields were determined by $^1$H NMR spectroscopy using cyclohexane as an internal standard. Errors were estimated to be ±2.5%. [c]Reaction was completed at room temperature in 10 min.

**Table 4. Aromatic C−H Borylation Using Different Olefins**[a]

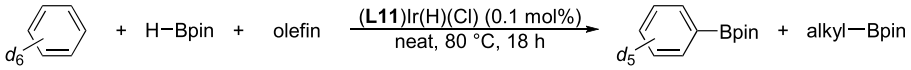


25 equiv 1 equiv 3 equiv

| entry | olefin | conversion[b] (%) | yield[b] (%) $C_6D_5Bpin$ | yield[b] (%) alkyl-Bpin |
|---|---|---|---|---|
| 1 | 1-hexene | 100 | 83 | 17 |
| 2 | *tert*-butylethylene (TBE) | 5 | 3 | 1 |
| 3 | *cis*-cyclooctene (COE) | 0 | 0 | 0 |
| 4 | norbornene | 14 | 10 | 3 |

[a]Reaction conditions: HBpin (36 $\mu$L, 0.25 mmol), (**L11**)Ir(H)(Cl) (0.27 $\mu$mol), $C_6D_6$ (550 $\mu$L, 6.21 mmol), olefin (0.74 mmol), 80 °C, under Ar, 18 h. [b]Conversions and yields were determined by $^1$H and/or $^{11}B\{^1H\}$ NMR spectroscopy using cyclohexane as a $^1$H internal standard. Errors were estimated to be ±2.5%.

**Table 5. Effect of Reagent Ratio on Product Ratio Using (L11)Ir(H)(Cl) as a Precatalyst**[a]

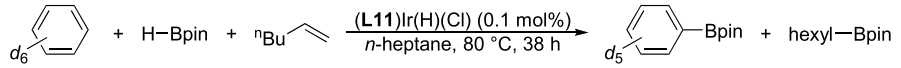


*X* equiv 1 equiv *Y* equiv

| entry | $C_6D_6$ (M) [*X*] | 1-hexene (M) [*Y*] | conversion[b] (%) | yield[b] (%) $C_6D_5Bpin$ | yield[b] (%) hexyl-Bpin |
|---|---|---|---|---|---|
| 1 | 1.7 [**5**] | 0.33 [**1**] | 33 | 23 | 9 |
| 2 | 1.7 [**5**] | 0.66 [**2**] | 100 | 72 | 28 |
| 3[c] | 1.7 [**5**] | 1.0 [**3**] | 100 | 64 | 36 |
| 4 | 8.4 [**25**] | 0.33 [**1**] | 47 | 40 | 6 |
| 5 | 8.4 [**25**] | 0.66 [**2**] | 100 | 86 | 14 |
| 6[c] | 8.4 [**25**] | 1.0 [**3**] | 100 | 83 | 17 |

[a]Reaction conditions unless specified otherwise: HBpin (70 $\mu$L, 0.48 mmol, 0.33 M), (**L11**)Ir(H)(Cl) (0.49 $\mu$mol), $C_6D_6$, 1-hexene in *n*-heptane, 80 °C, under Ar, 38 h. [b]Conversions and yields were determined by $^{11}B\{^1H\}$ NMR spectroscopy. Errors were estimated to be ±2.5%. [c]HBpin was consumed after 19 h.

precursors in aromatic C−H borylation that used HBpin as the boron reagent and required an olefin additive. The role of the olefin was studied in a previous publication for the prototypical catalysts based on the ligands **L1**−**L3**, where it was determined that the olefin is not merely a stoichiometric scavenger of the $H_2$ byproduct but is necessary to access the key unsaturated


https://doi.org/10.1021/acs.organomet.1c00081
*Organometallics* 2021, 40, 1004−1013

**Table 6. Regioselectivity Test for Aromatic C−H Borylation Experiments Using Ir Precatalysts**[a]

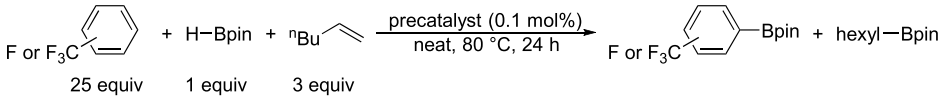


| entry | precatalyst | ArH | conversion (%)[b] | yield (%)[b] Ar-Bpin | yield (%)[b] hexyl-Bpin | *ortho/meta/para*[c] |
|---|---|---|---|---|---|---|
| 1 | (**L3**)Ir(H)(Cl) | PhF | 100 | 66 | 32 | 54/40/6 |
| 2 | (**L4**)Ir(H)(Cl) | PhF | 49 | 32 | 8 | 55/40/5 |
| 3 | (**L7**)Ir(H)(Cl) | PhF | 60 | 34 | 15 | 52/41/7 |
| 4 | (**L11**)Ir(H)(Cl) | PhF | 100 | 81 | 14 | 32/54/14 |
| 5 | (**L13**)Ir(H)(Cl) | PhF | 30 | 4 | 17 | 30/44/26 |
| 6 | (**L15**)Ir(H)(OAc) | PhF | 93 | 19 | 45 | 22/67/11 |
| 7 | (**L3**)Ir(H)(Cl) | $PhCF_3$ | 100 | 66 | 25 | 0/69/31 |
| 8 | (**L4**)Ir(H)(Cl) | $PhCF_3$ | 27 | 12 | 8 | 0/71/29 |
| 9 | (**L7**)Ir(H)(Cl) | $PhCF_3$ | 33 | 15 | 14 | 0/69/31 |
| 10 | (**L11**)Ir(H)(Cl) | $PhCF_3$ | 96 | 72 | 14 | 0/69/31 |
| 11 | (**L13**)Ir(H)(Cl) | $PhCF_3$ | 26 | 3 | 11 | 0/72/28 |
| 12 | (**L15**)Ir(H)(OAc) | $PhCF_3$ | 81 | 16 | 26 | 0/75/25 |

[a]Reaction conditions when PhF is used as the substrate: HBpin (62 μL, 0.43 mmol), 1-hexene (160 μL, 1.28 mmol), and precatalyst (0.45 μmol) in PhF (1.00 mL, 10.7 mmol), 80 °C, under Ar, for 24 h. Reaction conditions when $PhCF_3$ is used as the substrate: HBpin (48 μL, 0.33 mmol), 1-hexene (125 μL, 1.00 mmol), and precatalyst (0.34 μmol) in $PhCF_3$ (1.00 mL, 8.14 mmol), 80 °C, under Ar, for 24 h. [b]Conversions and yields were determined by $^1$H NMR spectroscopy using cyclohexane as an internal standard. Errors were estimated tb be ±2.5%. [c]Product ratios were determined by $^{19}$F NMR spectroscopy.

**Scheme 5. Chemoselectivity for sp$^2$ C−H, sp$^3$ C−H, and C−Cl Bonds**

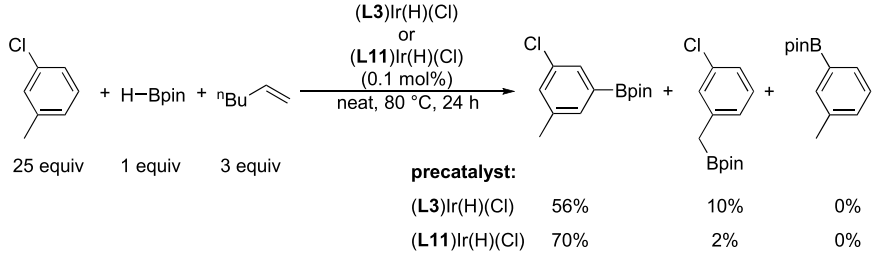


(pincer)Ir intermediate that is responsible for the C−H activation of the aromatic substrate.

In the present study, it was discovered that Rh pincer complexes were incapable of C−H borylation and only the Ir complexes of pincer ligands with a central aryl site displayed meaningful activity in C−H borylation. A comparison of the activity and the chemoselectivity (vs the competing olefin hydroboration) identified Ir complexes of the originally studied **L3** (POCOP-type) and the newly tested **L11** (PCP type) pincers as the most promising, with **L11** delivering a moderate improvement over **L3**. The regioselectivity of the C−H borylation in mono- and bis-substituted benzenes closely follows that observed in the "classical" Ir C−H borylation complexes supported by neutral bidentate phosphines or bipyridines. Since the mechanism of C−H borylation by Ir catalysts supported by pincer ligands is quite different, we conclude that the regioselectivity is substrate-controlled and reflects primarily a steric preference for C−H bonds without a neighboring *ortho* substituent.

## ■ ASSOCIATED CONTENT

### Supporting Information

The Supporting Information is available free of charge at https://pubs.acs.org/doi/10.1021/acs.organomet.1c00081.

Details of experimental procedures for the catalytic reactions, graphical NMR spectra, and details of X-ray structural determination (PDF)

### Accession Codes

CCDC 2041134 contains the supplementary crystallographic data for this paper. These data can be obtained free of charge via www.ccdc.cam.ac.uk/data_request/cif, or by emailing data_request@ccdc.cam.ac.uk, or by contacting The Cambridge Crystallographic Data Centre, 12 Union Road, Cambridge CB2 1EZ, UK; fax: +44 1223 336033.

## ■ AUTHOR INFORMATION


### Corresponding Author

**Oleg V. Ozerov** − *Department of Chemistry, Texas A&M University, College Station, Texas 77842, United States;* orcid.org/0000-0002-5627-1120; Email: ozerov@chem.tamu.edu

### Authors

**Ming-Uei Hung** − *Department of Chemistry, Texas A&M University, College Station, Texas 77842, United States*

**Loren P. Press** − *Department of Chemistry, Texas A&M University, College Station, Texas 77842, United States*

**Nattamai Bhuvanesh** − *Department of Chemistry, Texas A&M University, College Station, Texas 77842, United States*

Complete contact information is available at:

https://pubs.acs.org/10.1021/acs.organomet.1c00081

### Notes

The authors declare no competing financial interest.

## ■ ACKNOWLEDGMENTS

We are thankful for the support of this work by the US National Science Foundation (grant CHE-1565923 to O.V.O.). We acknowledge Melissa A. Schumacher and Dr. Morgan C. MacInnis for performing early experiments aimed at the synthesis of precursors to ligand **L15-H** and Dr. Samuel D. Timpa for preliminary work on **L6**. We are also grateful to Yihan Cao, Dr. Alex J. Kosanovich, and Dr. Qingheng Lai for the synthesis of some of the previously reported compounds used in this work.

## ■ REFERENCES

(1) Hall, D. G. *Boronic Acids: Preparation and Applications in Organic Synthesis, Medicine and Materials*, 2nd ed.; Wiley-VCH: Weinheim, Germany, 2012.
(2) Mkhalid, I. A. I.; Barnard, J. H.; Marder, T. B.; Murphy, J. M.; Hartwig, J. F. C−H Activation for the Construction of C-B Bonds. *Chem. Rev.* **2010**, *110*, 890−931.
(3) Hartwig, J. F. Borylation and Silylation of C−H Bonds: A Platform for Diverse C−H Bond Functionalizations. *Acc. Chem. Res.* **2012**, *45*, 864−873.
(4) Hartwig, J. F. Regioselectivity of the Borylation of Alkanes and Arenes. *Chem. Soc. Rev.* **2011**, *40*, 1992−2002.
(5) Hartwig, J. F. Evolution of C−H Bond Functionalization from Methane to Methodology. *J. Am. Chem. Soc.* **2016**, *138*, 2−24.
(6) Cho, J.-Y.; Tse, M. K.; Holmes, D.; Maleczka, R. E., Jr.; Smith, M. R., III Remarkably Selective Iridium Catalysts for the Elaboration of Aromatic C−H Bonds. *Science* **2002**, *295*, 305−308.
(7) Ishiyama, T.; Takagi, J.; Ishida, K.; Miyaura, N.; Anastasi, N. R.; Hartwig, J. F. Mild Iridium-Catalyzed Borylation of Arenes. High Turnover Numbers, Room Temperature Reactions, and Isolation of a Potential Intermediate. *J. Am. Chem. Soc.* **2002**, *124*, 390−391.
(8) Preshlock, S. M.; Ghaffari, B.; Maligres, P. E.; Krska, S. W.; Maleczka, R. E.; Smith, M. R., III High-Throughput Optimization of Ir-Catalyzed C−H Borylation: A Tutorial for Practical Applications. *J. Am. Chem. Soc.* **2013**, *135*, 7572−7582.
(9) Obligacion, J. V.; Semproni, S. P.; Chirik, P. J. Cobalt-Catalyzed C−H Borylation. *J. Am. Chem. Soc.* **2014**, *136*, 4133−4136.
(10) Schaefer, B. A.; Margulieux, G. W.; Small, B. L.; Chirik, P. J. Evaluation of Cobalt Complexes Bearing Tridentate Pincer Ligands for Catalytic C−H Borylation. *Organometallics* **2015**, *34*, 1307−1320.
(11) Obligacion, J. V.; Bezdek, M. J.; Chirik, P. J. C($sp^2$)-H Borylation of Fluorinated Arenes Using an Air-Stable Cobalt Precatalyst: Electronically Enhanced Site Selectivity Enables Synthetic Opportunities. *J. Am. Chem. Soc.* **2017**, *139*, 2825−2832.
(12) Obligacion, J. V.; Chirik, P. J. Mechanistic Studies of Cobalt-Catalyzed C($sp^2$)-H Borylation of Five-Membered Heteroarenes with Pinacolborane. *ACS Catal.* **2017**, *7*, 4366−4371.
(13) Furukawa, T.; Tobisu, M.; Chatani, N. C−H Functionalization at Sterically Congested Positions by the Platinum-Catalyzed Borylation of Arenes. *J. Am. Chem. Soc.* **2015**, *137*, 12211−12214.
(14) Dombray, T.; Werncke, C. G.; Jiang, S.; Grellier, M.; Vendier, L.; Bontemps, S.; Sortais, J.-B.; Sabo-Etienne, S.; Darcel, C. Iron-Catalyzed C−H Borylation of Arenes. *J. Am. Chem. Soc.* **2015**, *137*, 4062−4065.
(15) Mazzacano, T. J.; Mankad, N. P. Base Metal Catalysts for Photochemical C−H Borylation That Utilize Metal-Metal Cooperativity. *J. Am. Chem. Soc.* **2013**, *135*, 17258−17261.
(16) Legare, M.-A.; Courtemanche, M.-A.; Rochette, E.; Fontaine, F.-G. Metal-free catalytic C−H bond activation and borylation of heteroarenes. *Science* **2015**, *349*, 513−516.
(17) Chen, H.; Schlecht, S.; Semple, T. C.; Hartwig, J. F. Thermal, Catalytic, Regiospecific Functionalization of Alkanes. *Science* **2000**, *287*, 1995−1997.
(18) Murphy, J. M.; Lawrence, J. D.; Kawamura, K.; Incarvito, C.; Hartwig, J. F. Ruthenium-Catalyzed Regiospecific Borylation of Methyl C−H Bonds. *J. Am. Chem. Soc.* **2006**, *128*, 13684−13685.
(19) Chen, H.; Hartwig, J. F. Catalytic, Regiospecific End-Functionalization of Alkanes: Rhenium-Catalyzed Borylation under Photochemical Conditions. *Angew. Chem., Int. Ed.* **1999**, *38*, 3391−3393.
(20) Brown, J. M.; Lloyd-Jones, G. C. Vinylborane Formation in Rhodium-Catalyzed Hydroboration of Vinylarenes. Mechanism versus Borane Structure and Relationship to Silation. *J. Am. Chem. Soc.* **1994**, *116*, 866−868.
(21) Coapes, R. B.; Souza, F. E. S.; Thomas, R. L.; Hall, J. J.; Marder, T. B. Rhodium catalyzed dehydrogenative borylation of vinylarenes and 1,1-disubstituted alkenes without sacrificial hydrogenation - a route to 1,1-disubstituted vinylboronates. *Chem. Commun.* **2003**, 614−615.
(22) Ishiyama, T.; Ishida, K.; Takagi, J.; Miyaura, N. Palladium-Catalyzed Benzylic C−H Borylation of Alkylbenzenes with Bis(pinacolato)diboron or Pinacolborane. *Chem. Lett.* **2001**, *30*, 1082−1083.
(23) Olsson, V. J.; Szabó, K. J. Selective One-Pot Carbon-Carbon Bond Formation by Catalytic Boronation of Unactivated Cycloalkenes and Subsequent Coupling. *Angew. Chem., Int. Ed.* **2007**, *46*, 6891−6893.
(24) Larsen, M. A.; Cho, S. H.; Hartwig, J. F. Iridium-Catalyzed, Hydrosilyl-Directed Borylation of Unactivated Alkyl C−H Bonds. *J. Am. Chem. Soc.* **2016**, *138*, 762−765.
(25) Larsen, M. A.; Wilson, C. V.; Hartwig, J. F. Iridium-Catalyzed Borylation of Primary Benzylic C - H Bonds without a Directing Group: Scope, Mechanism, and Origins of Selectivity. *J. Am. Chem. Soc.* **2015**, *137*, 8633−8643.
(26) Lee, C.-I; Zhou, J.; Ozerov, O. V. Catalytic Dehydrogenative Borylation of Terminal Alkynes by a SiNN Pincer Complex of Iridium. *J. Am. Chem. Soc.* **2013**, *135*, 3560−3566.
(27) Zhou, J.; Lee, C.-I; Ozerov, O. V. Computational Study of the Mechanism of Dehydrogenative Borylation of Terminal Alkynes by SiNN Iridium Complexes. *ACS Catal.* **2018**, *8*, 536−545.
(28) Lee, C.-I; DeMott, J. C.; Pell, C. J.; Christopher, A.; Zhou, J.; Bhuvanesh, N.; Ozerov, O. V. Ligand Survey Results in Identification of PNP Pincer Complexes of Iridium as Long-lived and Chemoselective Catalysts for Dehydrogenative Borylation of Terminal Alkynes. *Chem. Sci.* **2015**, *6*, 6572−6582.
(29) Pell, C. J.; Ozerov, O. V. Synthesis and Rh-catalyzed reductive cyclization of 1,6-enynes and 1,6-diynes containing alkynylboronate termini. *J. Organomet. Chem.* **2020**, *912*, 121143.
(30) Foley, B. J.; Ozerov, O. V. Air- and Water-Tolerant (PNP)Ir Precatalyst for the Dehydrogenative Borylation of Terminal Alkynes. *Organometallics* **2020**, *39*, 2352−2355.
(31) Foley, B. J.; Bhuvanesh, N. S.; Zhou, J.; Ozerov, O. V. Combined Experimental and Computational Studies of the Mechanism of Dehydrogenative Borylation of Terminal Alkynes (DHBTA) Catalyzed by PNP Complexes of Iridium. *ACS Catal.* **2020**, *10*, 9824−9836.
(32) *The Chemistry of Pincer Compounds*; Morales-Morales, D., Jensen, C. M., Eds.; Elsevier: Amsterdam, The Netherlands, 2007.
(33) *Organometallic Pincer Chemistry*; van Koten, G., Milstein, D., Eds.; Springer: Heidelberg, Germany, 2013.
(34) Selander, N.; Szabó, K. J. Catalysis by Palladium Pincer Complexes. *Chem. Rev.* **2011**, *111*, 2048−2076.
(35) Kumar, A.; Bhatti, T. M.; Godman, A. S. Dehydrogenation of Alkanes and Aliphatic Groups by Pincer-Ligated Metal Complexes. *Chem. Rev.* **2017**, *117*, 12357−12384.
(36) Peris, E.; Crabtree, R. H. Key factors in pincer ligand design. *Chem. Soc. Rev.* **2018**, *47*, 1959−1968.
(37) Tsuchimoto, T.; Utsugi, H.; Sugiura, T.; Horio, S. Alkynylboranes: A Practical Approach by Zinc-Catalyzed Dehydrogenative Coupling of Terminal Alkynes with 1,8-Naphthalenediaminatoborane. *Adv. Synth. Catal.* **2015**, *357*, 77−82.

(38) Romero, E. A.; Jazzar, R.; Bertrand, G. Copper-catalyzed dehydrogenative borylation of terminal alkynes with pinacolborane. *Chem. Sci.* **2017**, *8*, 165−168.
(39) Wei, D.; Carboni, B.; Sortais, J.-B.; Darcel, C. Iron-Catalyzed Dehydrogenative Borylation of Terminal Alkynes. *Adv. Synth. Catal.* **2018**, *360*, 3649−3654.
(40) Procter, R. J.; Uzelac, M.; Cid, J.; Rushworth, P. J.; Ingleson, M. J. Low-coordinate NHC-Zinc Hydride Complexes Catalyze Alkyne C−H Borylation and Hydroboration Using Pinacolborane. *ACS Catal.* **2019**, *9*, 5760−5771.
(41) Pell, C. J.; Ozerov, O. V. Catalytic dehydrogenative borylation of terminal alkynes by POCOP-supported palladium complexes. *Inorg. Chem. Front.* **2015**, *2*, 720−724.
(42) Press, L. P.; Kosanovich, A. J.; McCulloch, B. J.; Ozerov, O. V. High-Turnover Aromatic C−H Borylation Catalyzed by POCOP-Type Pincer Complexes of Iridium. *J. Am. Chem. Soc.* **2016**, *138*, 9487−9497.
(43) Catalysis of aromatic C−H borylation by other pincer complexes had been reported, but those examples displayed only very modest activity likely because of the lack of the realization of the importance of a small sacrificial olefin in these systems, along with the limiting sterics of the pincer. (a) Fang, H.; Choe, Y. K.; Li, Y.; Shimada, S. Synthesis, Structure, and Reactivity of Hydridoiridium Complexes Bearing a Pincer-Type PSiP Ligand. *Chem. - Asian J.* **2011**, *6*, 2512−2521. (b) Bruck, A.; Gallego, D.; Wang, W.; Irran, E.; Driess, M.; Hartwig, J. F. Pushing the $\sigma$-Donor Strength in Iridium Pincer Complexes: Bis(silylene) and Bis(germylene) Ligands Are Stronger Donors than Bis(phosphorus(III)) Ligands. *Angew. Chem., Int. Ed.* **2012**, *51*, 11478−11482.
(44) Göttker-Schnetmann, I.; White, P.; Brookhart, M. Iridium Bis(phosphinite) *p*-XPCP Pincer Complexes: Highly Active Catalysts for the Transfer Dehydrogenation of Alkanes. *J. Am. Chem. Soc.* **2004**, *126*, 1804−1811.
(45) Ozerov, O. V.; Guo, C.; Foxman, B. M. Missing Link: PCP Pincer Ligands Containing P-N Bonds and Their Pd Complexes. *J. Organomet. Chem.* **2006**, *691*, 4802−4806.
(46) Murugesan, S.; Stöger, B.; Carvalho, M. D.; Ferreira, L. P.; Pittenauer, E.; Allmaier, G.; Veiros, L. F.; Kirchner, K. Synthesis and Reactivity of Four- and Five-Coordinate Low-Spin Cobalt(II) PCP Pincer Complexes and Some Nickel(II) Analogues. *Organometallics* **2014**, *33*, 6132−6140.
(47) Shih, W.-C.; Ozerov, O. V. One-Pot Synthesis of 1,3-Bis(phosphinomethyl)arene PCP/PNP Pincer Ligands and Their Nickel Complexes. *Organometallics* **2015**, *34*, 4591−4597.
(48) Pell, C. J.; Ozerov, O. V. A Series of Pincer-Ligated Rhodium Complexes as Catalysts for the Dimerization of Terminal Alkynes. *ACS Catal.* **2014**, *4*, 3470−3480.
(49) Fan, L.; Foxman, B. M.; Ozerov, O. V. N-H Cleavage as a Route to Palladium Complexes of a New PNP Pincer Ligand. *Organometallics* **2004**, *23*, 326−328.
(50) Kosanovich, A. J.; Jordan, A. M.; Bhuvanesh, N.; Ozerov, O. V. Synthesis and Characterization of Rhodium, Iridium, and Palladium Complexes of a Diarylamido-based PNSb Pincer Ligand. *Dalton Trans.* **2018**, *47*, 11619−11624.
(51) Shih, W.-C.; Gu, W.; MacInnis, M. C.; Timpa, S. D.; Bhuvanesh, N.; Zhou, J.; Ozerov, O. V. Facile Insertion of Rh and Ir into a Boron-Phenyl Bond, Leading to Boryl/Bis(phosphine) PBP Pincer Complexes. *J. Am. Chem. Soc.* **2016**, *138*, 2086−2089.
(52) Timpa, S. D.; Zhou, J.; Bhuvanesh, N.; Ozerov, O. V. Potential Carbon-Fluorine Reductive Elimination from Pincer-Supported Rh(III) and Dominating Side Reactions: Theoretical and Experimental Examination. *Organometallics* **2014**, *33*, 6210−6217.
(53) Weng, W.; Guo, C.; Çelenligil-Çetin, R.; Foxman, B. M.; Ozerov, O. V. Skeletal Change in the PNP Pincer Ligand Leads to a Highly Regioselective Alkyne Dimerization Catalyst. *Chem. Commun.* **2006**, 197−199.
(54) Ozerov, O. V.; Guo, C.; Papkov, V. A.; Foxman, B. M. Facile Oxidative Addition of N-C and N-H Bonds to Monovalent Rhodium and Iridium. *J. Am. Chem. Soc.* **2004**, *126*, 4792−4793.
(55) Shih, W.-C.; Ozerov, O. V. Synthesis and Characterization of PBP Pincer Iridium Complexes and Their Application in Alkane Transfer Dehydrogenation. *Organometallics* **2017**, *36*, 228−233.
(56) Timpa, S. D.; Fafard, C. M.; Herbert, D. E.; Ozerov, O. V. Catalysis of Kumada-Tamao-Corriu Coupling by a ($P^OC^OP$)Rh Pincer Complex. *Dalton Trans.* **2011**, *40*, 5426−5429.
(57) Mucha, N. T.; Waterman, R. Iridium Pincer Catalysts for Silane Dehydrocoupling: Ligand Effects on Selectivity and Activity. *Organometallics* **2015**, *34*, 3865−3872.
(58) (**L17**)Ir(COE) was afforded by reacting the ligand precursor **L17-H** with $NaN(SiMe_3)_2$, followed by $[(COE)_2IrCl]_2$, which has been described in ref 50.
(59) A reaction of ligand precursor **L18-Ph** and $[(COE)_2IrCl]_2$ led to (**L18**)Ir(Ph)(Cl). (**L18**)$Ir(H)_4$ can be afforded by treating (**L18**)Ir(Ph)(Cl) with $H_2$, followed by $NaEt_3BH$ under $H_2$, which has been described in ref 55.
(60) Farrugia, L. J. J. *ORTEP* −3 for Windows - A Version of *ORTEP* -III with a Graphical User Interface (GUI). *J. Appl. Crystallogr.* **1997**, *30*, 565−565.


https://doi.org/10.1021/acs.organomet.1c00081
*Organometallics* 2021, 40, 1004−1013